

## Intersubband optical absorption in heavily doped *n*-type GaAs/Al<sub>0.3</sub>Ga<sub>0.7</sub>As multiple quantum wells

B. Jogai

*University Research Center, Wright State University, Dayton, Ohio 45435*

M. O. Manasreh and C. E. Stutz

*Solid State Electronics Directorate (WL/ELRA), Wright Laboratory, Wright-Patterson Air Force Base, Ohio 45433-6543*

R. L. Whitney and D. K. Kinell

*Lockheed Palo Alto Research Laboratories, Palo Alto, California 94304-1191*

(Received 11 May 1992)

Intersubband optical absorption between the ground and first excited states and the first and second excited states is reported for *n*-type doped GaAs/Al<sub>1-x</sub>Ga<sub>x</sub>As multiple quantum wells. This phenomenon is shown to be due to high doping, which causes more than one subband to be populated. Experimental results supported by theoretical calculations are presented.

### I. INTRODUCTION

Recently, there has been an increasing interest in the intersubband transitions in III-V and IV-IV semiconductor multiple quantum wells (MQW's).<sup>1-11</sup> This is mainly because of their use in long-wavelength infrared detection. GaAs/Al<sub>x</sub>Ga<sub>1-x</sub>As multiple quantum wells have been extensively studied for applications in the 8-12- $\mu$ m spectral region. Photon absorption in this class of detectors is achieved by doping the quantum well with a donor species such as Si so that the ground state in the conduction subband is partially filled with electrons that can be promoted to a higher energy level by the incoming photons.

To date, all of the published works for GaAs/Al<sub>x</sub>Ga<sub>1-x</sub>As quantum wells have reported transitions between the ground and first excited electron states. In this paper, we report both ground-to-excited-state and excited-to-excited-state transitions in doped GaAs/Al<sub>x</sub>Ga<sub>1-x</sub>As multiple quantum wells. Similar results have been reported for unstrained In<sub>x</sub>Ga<sub>1-x</sub>As/In<sub>x</sub>Al<sub>1-x</sub>As multiple quantum wells.<sup>12,13</sup> The interpretation of the results is supported by a theoretical model that includes many-body effects.

### II. EXPERIMENTAL PROCEDURE

Two samples were grown for this study. The first, Sample 1, consists of 100 periods of 75- $\text{\AA}$  Si-doped GaAs wells separated by 100- $\text{\AA}$  Al<sub>0.3</sub>Ga<sub>0.7</sub>As barriers. The wells are uniformly doped with a density of  $10^{18} \text{ cm}^{-3}$ . The second, Sample 2, is identical in geometry to the first, except that the Si concentration is  $\sim 8 \times 10^{18} \text{ cm}^{-3}$ . The optical-absorption spectra were recorded using a BOMEM interferometer. The incident beam was directed at the Brewster angle so that some of the refracted light would propagate in the in-plane direction. The samples were cooled to liquid nitrogen temperature. Spectra were also recorded at room temperature.

### III. METHOD OF CALCULATION

We have calculated the intersubband energy differences of these samples to determine whether all of the peaks can be explained by intersubband electron transitions, or whether an alternative process, perhaps impurity-state transitions, is responsible for some peaks. Because the samples are heavily doped, the Coulomb interaction is expected to be significant enough to modify the band edge so that it deviates from flatband. Consequently, the calculation must be self-consistent. The model is explained in detail in Ref. 14. Briefly, the eigenstates are calculated from a four-band  $\mathbf{k} \cdot \mathbf{p}$  formulation, and, provided that the Fermi level is known, the free-electron density is calculated from the resulting wave functions by employing Fermi-Dirac statistics. The Fermi level is obtained iteratively by invoking the charge-neutrality condition: we assume that each period of the MQW is electrically neutral. We also assume that all of the Si donors are ionized at all temperatures, an approximation that seems reasonable for bulk GaAs, but one that has not been tested for quantum wells. From the charge distribution, both the Hartree and exchange-correlation parts of the Coulomb interaction are calculated. The former is obtained from the Poisson equation and the latter from density-functional theory within the local-density approximation.<sup>15</sup> The explicit temperature dependence of the exchange-correlation potential is not included. The corrected potential energy is fed to the  $\mathbf{k} \cdot \mathbf{p}$  Hamiltonian and the entire process repeated until the potential converges, i.e., until the maximum change between successive steps is negligible. Additional many-body effects need to be included to correctly model the absorption process. In general, the absorption peak does not occur at the exact energy separation between a given pair of states. When the incoming photon is near the energy of a given intersubband separation, oscillations are resonantly induced in the electron gas. Additional energy, approximately equal to that of a plasmon mode, is then needed to promote an electron to a higher state. This effect, known as depolarization, is included in the final results. Also included is

the vertex correction or excitonlike binding energy between the excited electron and the “hole” left behind. This effect produces a redshift.

If we take the foregoing effects into account, the absorption energy is given by<sup>16</sup>

$$\bar{E}_{if} = E_{if} \sqrt{1+a-b}, \quad (1)$$

where  $E_{if}$  is the self-consistently calculated energy separation between the initial state  $i$  and final state  $f$  and  $a$  and  $b$  are the depolarization and vertex corrections, respectively. Assuming a two-level system, the absorption coefficient is found from<sup>17</sup>

$$\alpha(\omega) = \left[ \frac{\mu_0 c}{n_r} \right] \left[ \frac{\pi e^2 \hbar}{2m_0} \right] s_{if} J_{if}, \quad (2a)$$

where

$$s_{if} = \left[ \frac{2}{m_0 \hbar \omega} \right] |M_{if}|^2 \quad (2b)$$

and

$$J_{if} = \left[ \frac{m^*}{2\pi^3 \hbar^2 L} \right] \frac{\Gamma}{(\bar{E}_{if} - \hbar\omega)^2 + \Gamma^2} \int dE_{\parallel} f_i(1-f_f), \quad (2c)$$

in which  $\mu_0$  is the free-space permeability,  $c$  is the speed of light,  $n_r$  is the refractive index,  $m_0$  is the free-electron mass,  $L$  is the period of the multiple quantum well,  $M_{if}$  is the momentum matrix element between the initial and final states,  $f_i$  and  $f_f$  are the Fermi-Dirac functions for the initial and final states, respectively,  $E_{\parallel}$  is the energy in the in-plane direction, and  $\Gamma$  is a temperature-dependent collision-broadening parameter. The quantities defined in Eqs. (2b) and (2c) are the oscillator strength and joint density of states, respectively. It is recommended that for intersubband transitions,<sup>18</sup>  $m_0$  in Eqs. (2a) and (2b) be replaced *ad hoc* by  $m^*$ , the effective electron mass. Although not rigorously established, we find that the calculated absorption coefficient would be two orders of magnitude too small if this substitution were not made.

#### IV. RESULTS AND DISCUSSION

Figure 1(a) shows the experimental spectra for Sample 1 obtained at room temperature and 77 K. Figure 1(b) shows the calculated eigenstates, conduction-band edge, and electron distribution for this sample. The subband pairs likely to cause absorption have the following theoretical energy separations:  $E_{12} = 125.3$  meV,  $E_{13}$

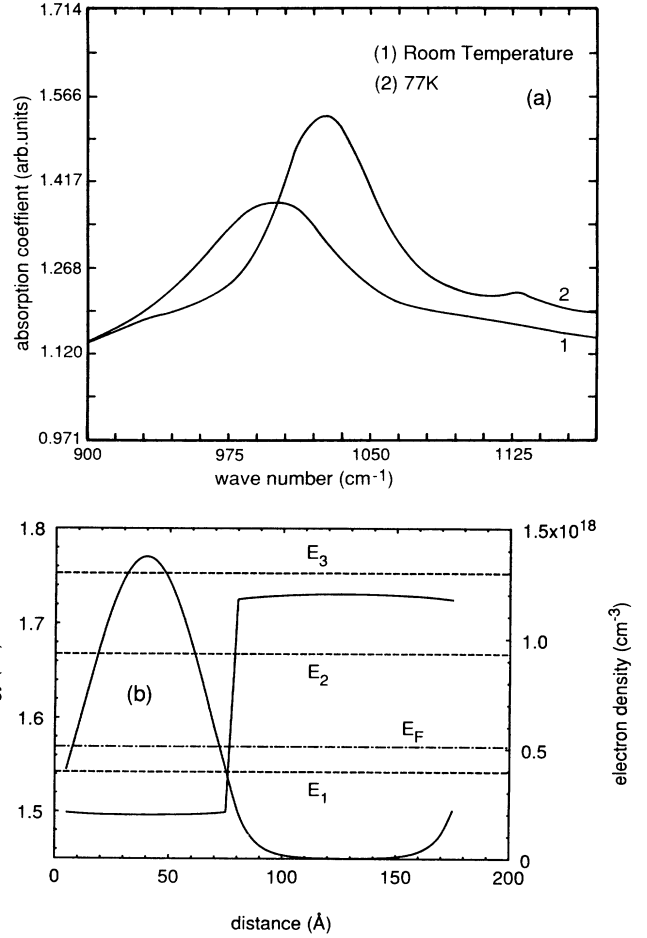


FIG. 1. (a) Measured absorption coefficient at 77 and 300 K for Sample 1. (b) Calculated conduction-band edge (left-hand y axis) and electron density (right-hand y axis) at 77 K for Sample 1. The first few subband energies (dashed lines) and the Fermi level (dot-dashed line) are plotted against the left-hand y axis.

$= 210.5$  meV, and  $E_{23} = 85.2$  meV. The Fermi level is 26.7 meV above  $E_1$ . Of these subband pairs,  $E_{12}$  is closest to the measured results. (See Table I). We predict an absorption peak, i.e., the transition energy between  $E_1$  and  $E_2$  corrected for the depolarization and vertex effects, at 126.8 meV. Thus, the combined depolarization and vertex effects produce a 1-meV blueshift. From Fig. 1(a), the measured peak is at 127.4 meV and is in good agreement with the predicted value. The calculation reveals that  $J_{if}$  for the  $E_1 \rightarrow E_2$  and  $E_1 \rightarrow E_3$  transitions is comparable in magnitude, but that of  $E_2 \rightarrow E_3$  is about

TABLE I. Calculated intersubband parameters and measured peak energies for the two samples. The quantities  $s_{if}$ ,  $J_{if}$ , and  $\alpha$  are defined in Eq. (2).

Transitions	Sample 1						Sample 2					
	$E_{if}$ (meV)	$\bar{E}_{if}$ (meV)	Peak expt. (meV)	$s_{if}$	$J_{if}$ ( $\text{eV}^{-1} \text{cm}^{-3}$ )	$\alpha$ ( $\text{cm}^{-1}$ )	$E_{if}$ (meV)	$\bar{E}_{if}$ (meV)	Peak expt. (meV)	$s_{if}$	$J_{if}$ ( $\text{eV}^{-1} \text{cm}^{-3}$ )	$\alpha$ ( $\text{cm}^{-1}$ )
$E_1 \rightarrow E_2$	125.3	126.8	127.4	0.93	$6.0 \times 10^{18}$	2498	126.9	153.7	144.8	0.82	$1.2 \times 10^{19}$	4496
$E_1 \rightarrow E_3$	210.5	211.4		$6.69 \times 10^{-4}$	$6.0 \times 10^{18}$	1.8	220.3	233.2		$1.08 \times 10^{-3}$	$1.1 \times 10^{19}$	8.5
$E_2 \rightarrow E_3$	85.2	82.1		2.41	$5.4 \times 10^{11}$	$2 \times 10^{-4}$	93.4	101.2	112.7	2.33	$5.3 \times 10^{18}$	5559

seven orders of magnitude smaller. These results are summarized in Table I. In calculating  $J_{if}$  from Eq. (2c), we estimated  $\Gamma$  from the half-width at half maximum of the measured peak, yielding  $\Gamma=3.6$  meV. An *ab initio* determination of  $\Gamma$  is beyond the scope of the present work.

If we approximate the areal electron density in the  $i$ th subband by

$$n_i^{2D} = \frac{m^* kT}{\pi \hbar^2} \ln \left[ 1 + \exp \left( \frac{E_F - E_i}{kT} \right) \right], \quad (3)$$

we find that  $n_1^{2D} = 7.5 \times 10^{11} \text{ cm}^{-2}$  at 77 K for Sample 1. Accordingly, all of the electrons reside in  $E_1$ . For this sample, excited-to-excited-state transitions are unlikely. Indeed, for this sample, only one peak was observed, even though a wide range of wavelengths was scanned. Although electrons are available for  $E_1 \rightarrow E_3$  transitions, the oscillator strength  $s_{if}$  is about three orders of magnitude smaller than that of  $E_1 \rightarrow E_2$  or  $E_2 \rightarrow E_3$ . (See Table I.) An overall measure of whether a peak can be observed is the absorption coefficient. This quantity is substantially larger for  $E_1 \rightarrow E_2$  than for  $E_1 \rightarrow E_3$  or  $E_2 \rightarrow E_3$ . These values are consistent with the observation of only one peak. The theoretical peak absorption coefficient, shown in Table I, compares favorably with the measured peak of  $1863 \text{ cm}^{-1}$ .

In Fig. 2(a), we show the experimental spectra for Sample 2 recorded at room temperature and 77 K. The corresponding theoretical results are shown in Fig. 2(b). Here we find  $E_{12} = 126.9$  meV,  $E_{13} = 220.3$  meV, and  $E_{23} = 93.4$  meV. Corrected for the depolarization and vertex effects, the transition energies become  $\bar{E}_{12} = 153.7$  meV,  $\bar{E}_{13} = 233.2$  meV, and  $\bar{E}_{23} = 101.2$  meV. The Fermi level is 170.9 meV above  $E_1$  and 44 meV above  $E_2$ . The position of the Fermi level ensures that at least two states are occupied. From Eq. (3), the areal electron densities in the first three subbands are given by  $n_1^{2D} = 4.77 \times 10^{12} \text{ cm}^{-2}$ ,  $n_2^{2D} = 1.23 \times 10^{12} \text{ cm}^{-2}$ , and  $n_3^{2D} = 1.09 \times 10^8 \text{ cm}^{-2}$ . Based on these results, we strongly feel that the lower energy peak [i.e., the left peak in Fig. 2(a)] in the experimental data is attributable to  $E_2 \rightarrow E_3$  transitions and the higher one [the right peak in Fig. 2(a)] to  $E_1 \rightarrow E_2$  transitions. As Fig. 2(b) indicates,  $E_3$  is a virtual state above the  $\text{Al}_{0.3}\text{Ga}_{0.7}\text{As}$  barrier. To our knowledge, this is the first reported observation of excited-to-excited-state intersubband transitions in symmetrical  $\text{GaAs}/\text{Al}_x\text{Ga}_{1-x}\text{As}$  quantum wells. No other peaks were observed experimentally, despite scanning the energy in the 50–350-meV range. Although the joint density of states favors  $E_1 \rightarrow E_3$  transitions, the oscillator strength is about three orders of magnitude smaller than for the other two cases. These results are shown in Table I. The measured absorption coefficients for the left and right peaks are  $266.6$  and  $186.7 \text{ cm}^{-1}$ , respectively, and are significantly lower than the calculated values. A possible reason for the discrepancy is that when there are two peaks fairly close together, the absorption measured by Fourier transform infrared is not truly representative of  $\alpha$ . This is because the source beam excites all possible transitions simultaneously. The number of elec-

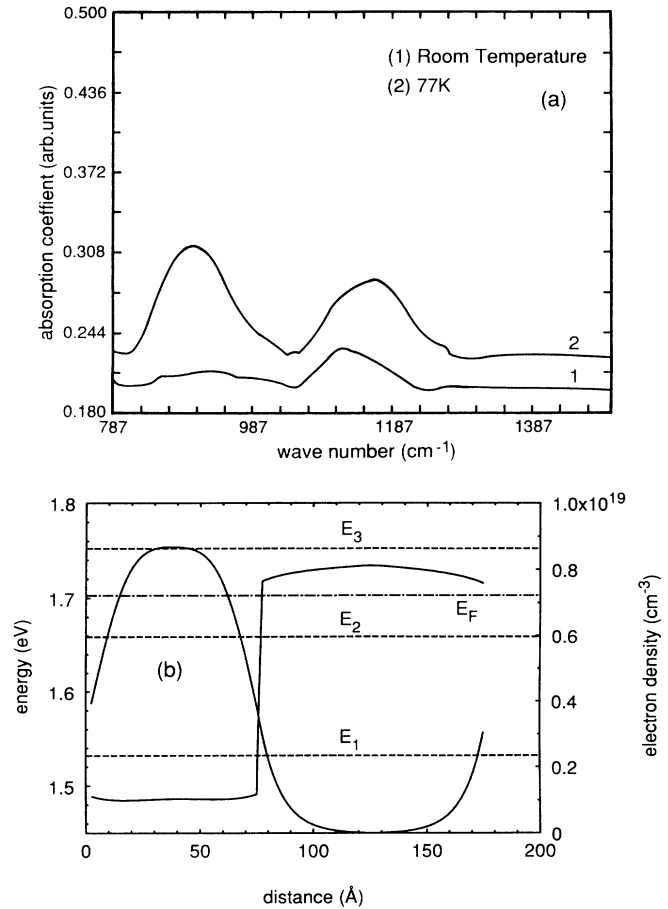


FIG. 2. (a) Measured absorption coefficient at 77 and 300 K for Sample 2. (b) Calculated results at 77 K for Sample 2. Axis designations are the same as in Fig. 1(b).

trons involved in the transitions will be less than the static electron density [Eq. (3)]. The calculated  $\alpha$ , however, is consistent with the first peak being higher than the second, as well as the absence of a peak attributable to  $E_1 \rightarrow E_3$ . The calculations show that band-filling effects do not eliminate the  $E_1 \rightarrow E_2$  transition; the joint density of states remains large for this transition. The two peaks observed in Fig. 2(a) were found to be repeatable in other samples grown under similar conditions as those of Sample 2. Other heavily doped  $\text{GaAs}/\text{Al}_x\text{Ga}_{1-x}\text{As}$  structures grown by us also show two intersubband transitions peaks. The presence of two intersubband transitions may have applications in multicolor long-wavelength infrared detectors.

The calculated  $\bar{E}_{if}$  for Sample 2 is not as close to experiment as for Sample 1. One source of error is that the dopant density in Sample 2 is difficult to estimate from the optical measurements. Additionally, deviations of the well width from the nominal width may also contribute to the discrepancy. If we increase the well width by 5 Å ( $\sim 2$  monolayers), we find  $\bar{E}_{12} = 148.7$  meV and  $\bar{E}_{23} = 110.9$  meV. These theoretical peaks are closer to the experimental results.

To verify that the peaks in the Sample 2 data were not due to processes other than intersubband transitions, for example, neutral-donor-to-subband transitions, we also

measured the spectra for normal incidence. In that case, no peaks were observed. The results were also repeatable: samples grown at different times by the same molecular-beam-epitaxy (MBE) system produced similar results, as did samples grown by a different MBE system. An interesting trend consistent with the foregoing interpretation was observed. If the dopant density was high enough to raise the Fermi level above two subbands, two peaks were always observed.

The difference between the two samples in the energy of the  $E_1 \rightarrow E_2$  transition clearly shows the importance of the depolarization and vertex effects for heavily-doped samples. Without these corrections, the predicted peaks would occur approximately at the same energy. For the second sample, depolarization causes a blueshift of 31 meV. Considered together, the two effects produce an overall blueshift of 27 meV. Despite the identical geometry of the two samples,  $E_{12}$  of Sample 2 is much larger than  $E_{12}$  of Sample 1. This difference is attributed to the variation of the dopant concentration, as shown in the present and previous<sup>19</sup> calculations and measurements.

For Sample 2, the peak attributed to  $E_2 \rightarrow E_3$  broadens as the temperature increases and almost disappears at 300 K. We have verified that this is not caused by the Fermi level dropping below  $E_2$  at higher temperatures. Figure 3 shows the variation of the Fermi level relative to  $E_1$  and  $E_2$  as a function of temperature. The separation decreases by only 4 meV as the temperature approaches 300 K. The population of  $E_2$  increases slightly, while that of  $E_1$  decreases correspondingly.

## V. SUMMARY

In conclusion, we have observed two peaks in the absorption spectra of heavily-doped GaAs/Al<sub>x</sub>Ga<sub>1-x</sub>As

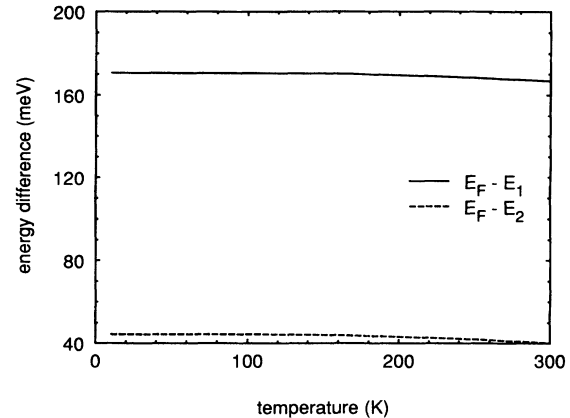


FIG. 3. Energy difference between the Fermi level and the populated states as a function of temperature.

MQW's. These peaks are attributed to ground-to-excited-state and excited-to-excited-state transitions and are caused by the Fermi level being above two states. The present interpretation is supported by a self-consistent  $\mathbf{k} \cdot \mathbf{p}$  calculation of the eigenstates that includes the many-body effects of Hartree, exchange correlation, depolarization, and vertex. These results may have applications in multicolor long-wavelength infrared detection.

## ACKNOWLEDGMENTS

This work is partially supported by the Air Force Office of Scientific Research. B.J. is supported under Contract No. F33615-91C-1765. The authors are grateful to J. Ehret and E. Taylor for MBE growth.

<sup>1</sup>M. O. Manasreh, *Quantum Structures for Long Wavelength Infrared Detectors* (Artech House, Norwood, MA, in press).

<sup>2</sup>B. F. Levine, K. K. Choi, C. G. Bethea, J. Walker, and R. J. Malik, *Appl. Phys. Lett.* **50**, 1092 (1987).

<sup>3</sup>B. F. Levine, C. G. Bethea, K. K. Choi, J. Walker, and R. J. Malik, *Appl. Phys. Lett.* **53**, 231 (1988).

<sup>4</sup>B. F. Levine, G. Hasnain, C. G. Bethea, and N. Chand, *Appl. Phys. Lett.* **54**, 2704 (1989).

<sup>5</sup>B. F. Levine, C. G. Bethea, G. Hasnain, V. O. Shen, E. Pelve, R. R. Abbott, and S. J. Hsieh, *Appl. Phys. Lett.* **56**, 851 (1990).

<sup>6</sup>R. J. Turton and M. Jaros, *Appl. Phys. Lett.* **56**, 767 (1990).

<sup>7</sup>C. I. Chang, D. S. Pan, and R. Somoano, *J. Appl. Phys.* **65**, 3253 (1989).

<sup>8</sup>Y. Rajakarunayake and T. C. McGill, *J. Vac. Sci. Technol. B* **8**, 929 (1990).

<sup>9</sup>R. P. G. Karunasiri, J. S. Park, K. L. Wang, and L. J. Cheng,

*Appl. Phys. Lett.* **56** 1342 (1990).

<sup>10</sup>R. P. G. Karunasiri, J. S. Park, Y. J. Mii, and K. L. Wang, *Appl. Phys. Lett.* **57**, 2585 (1990).

<sup>11</sup>R. People, *Phys. Rev. B* **32**, 1405 (1985).

<sup>12</sup>H. Asai and Y. Kawamura, *Appl. Phys. Lett.* **56**, 1427 (1990).

<sup>13</sup>H. Asai and Y. Kawamura, *Phys. Rev. B* **43**, 4748 (1991).

<sup>14</sup>B. Jogai, *J. Vac. Sci. Technol. B* **9**, 2473 (1991).

<sup>15</sup>L. Hedin and B. I. Lundqvist, *J. Phys. C* **4**, 2064 (1971).

<sup>16</sup>T. Ando, *Solid State Commun.* **21**, 133 (1977).

<sup>17</sup>K. Seeger, *Semiconductor Physics*, 3rd ed. (Springer-Verlag, Berlin, 1985).

<sup>18</sup>G. Bastard, *Wave Mechanics Applied to Semiconductor Heterostructures* (Les Éditions de Physique, Paris, 1988), Chap. 7, p. 242.

<sup>19</sup>M. O. Manasreh, F. Szmulowicz, T. Vaughan, K. R. Evans, C. E. Stutz, and D. W. Fischer, *Phys. Rev. B* **43**, 9996 (1991).